GEOLOGY | THE GEOLOGICAL SOCIETY OF AMERICA®

https://doi.org/10.1130/G47509.1

Manuscript received 26 November 2019
Revised manuscript received 6 May 2020
Manuscript accepted 8 May 2020

Direct coupling between carbon release and weathering during the Toarcian oceanic anoxic event

David B. Kemp[1], David Selby[2,3] and Kentaro Izumi[4]
[1]School of Earth Sciences, China University of Geosciences, Wuhan 430074, P.R. China
[2]Department of Earth Sciences, Durham University, Durham DH1 3LE, UK
[3]State Key Laboratory of Geological Processes and Mineral Resources, China University of Geosciences, Wuhan 430074, P.R. China
[4]Faculty and Graduate School of Education, Chiba University, 1-33 Yayoi-cho, Inage-ku, Chiba-shi, Chiba 263-8522, Japan

ABSTRACT

Silicate weathering represents a major feedback mechanism in the Earth's climate system, helping to stabilize atmospheric CO_2 levels and temperature on million-year time scales. On shorter time scales of greater relevance to understanding the fate of anthropogenic CO_2, the efficacy and responsiveness of weathering is less clear. Here, we present high-resolution osmium-isotope data that reflect global chemical weathering from a stratigraphically thick record of the early Toarcian oceanic anoxic event (T-OAE; ca. 182 Ma). A pronounced decrease in the carbon-isotope composition of exogenic carbon reservoirs during this event has been linked to the large-scale release of ^{12}C-enriched carbon. Our data indicate that the flux of radiogenic osmium to the oceans increased in lockstep with the decrease in carbon-isotope values, demonstrating a geologically synchronous coupling between massive carbon release and enhanced global continental crust weathering. We show that abrupt shifts in carbon isotopes, previously interpreted as millennial-scale methane hydrate melting or terrestrial carbon-release events, are coeval with rapid increases in weathering. Global weathering may have increased by >40% across each of these intervals of rapid carbon injection. Our results help to reconcile previous estimates of weathering change during the T-OAE, and support the view that, overall, global weathering rates may have increased six-fold through the entire event.

INTRODUCTION

Determining the response time and mechanistic links between rapid, large-scale climate change and weathering in deep time is challenging because of the typically low temporal resolution of geological records of climate change and the need for proxies that can unambiguously track globally significant changes in weathering on short time scales. The early Toarcian oceanic anoxic event (T-OAE; ca. 182 Ma) represents an ideal interval for studying weathering responses to inferred large-scale atmospheric CO_2 and temperature change. A pronounced decrease in the carbon-isotope ($\delta^{13}C$) composition of exogenic reservoirs through this event, coupled with associated evidence for seawater warming and atmospheric CO_2 increase, has been linked to the release of thousands of gigatons of ^{12}C-rich carbon to the biosphere (Hesselbo et al., 2000; McElwain et al., 2005; Kemp et al., 2005; Ruebsam et al., 2019).

Osmium-isotope ($^{187}Os/^{188}Os$) data from a handful of previous studies have demonstrated that the flux of radiogenic ^{187}Os derived from continental crust weathering increased significantly during the T-OAE (Cohen et al., 2004; Percival et al., 2016; Them et al., 2017a; van Acken et al., 2019). Nevertheless, the precise timing and pattern of this increase, and its exact relationship to inferred carbon release, are uncertain. In particular, the decrease to minimum $\delta^{13}C$ values has been shown to comprise a series of abrupt shifts, each likely reflecting millennial-scale carbon injection from methane hydrate or terrestrial wetland and/or permafrost sources (Kemp et al., 2005; Hesselbo and Pieńkowski, 2011; Them et al., 2017b; Izumi et al., 2018a; Ruebsam et al., 2019). The weathering response to these rapid injections is unclear. Furthermore, the overall magnitude of weathering change across the T-OAE is uncertain because Os-isotope values presented in the previous studies differ. In this study, we address these issues with a new high-resolution Os-isotope record through an expanded sedimentary succession of the T-OAE from Japan.

MATERIALS AND METHODS

To reconstruct the Os-isotope composition of contemporaneous seawater through the T-OAE ($^{187}Os/^{188}Os_i$; i—initial), we analyzed lower Toarcian organic-rich mudrocks exposed at Sakuraguchi-dani, Japan (34°08′N, 131°03′E), that were deposited on the margin of Panthalassa (Fig. 1). Previous organic carbon-isotope ($\delta^{13}C_{org}$) analysis at Sakuraguchi-dani has revealed a >35 m record of the T-OAE negative carbon-isotope excursion (CIE; Izumi et al., 2012, 2018a; Kemp and Izumi, 2014; Fig. 2). We selected 24 samples for Os-isotope analysis spanning the T-OAE and extending into the Pliensbachian. Abundances of detrital elements Al, Ti, and Zr were also quantified on these samples using X-ray fluorescence (XRF) analysis. For 11 samples, $\delta^{13}C_{org}$ was measured to supplement previously published data. Full details of the methods used for rhenium and osmium extraction, purification, and analysis and XRF and $\delta^{13}C$ analysis, and all data, are in the Supplemental Material[1].

RESULTS

The lower part of the Sakuraguchi-dani succession (–27.12 m to –9.47 m) is below the T-OAE negative CIE, and is characterized by extremely unradiogenic (^{188}Os-enriched) $^{187}Os/^{188}Os_i$ (~0.17), except for the lowermost

[1]Supplemental Material. Description of methods, Table S1, and Figures S1 and S2. Please visit https://doi.org/10.1130/GEOL.S.12425333 to access the supplemental material, and contact editing@geosociety.org with any questions.

CITATION: Kemp, D.B., Selby, D., and Izumi, K., 2020, Direct coupling between carbon release and weathering during the Toarcian oceanic anoxic event: Geology, v. 48, p. , https://doi.org/10.1130/G47509.1

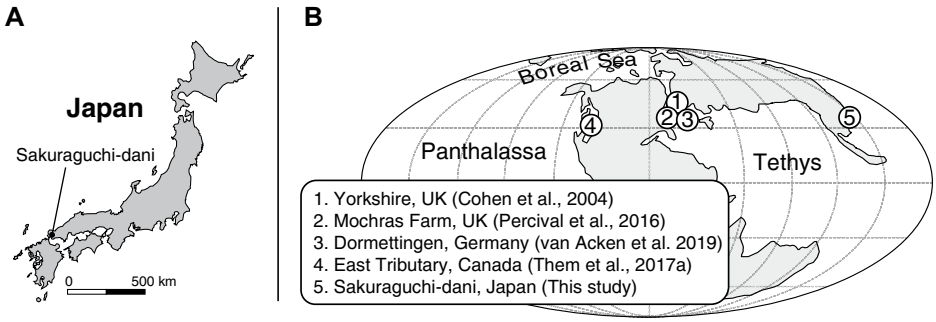

Figure 1. Maps showing modern location (A; 34°08′N, 131°03′E) and paleogeographic (B; ca. 182 Ma) location of the Sakuraguchi-dani site, Japan, and locations of previous early Toarcian Os-isotope studies (see Fig. 3). East Tributary refers to the East Tributary of Bighorn Creek. Redrawn from Izumi et al. (2012).

sample ($^{187}Os/^{188}Os_i$ = 0.47; Fig. 2A). Above –9.47 m and through the onset of the CIE, $^{187}Os/^{188}Os_i$ increases, reaching a maximum of 0.58 at 1.45 m height (Fig. 2A). Above this level, $^{187}Os/^{188}Os_i$ varies between 0.34 and 0.53 over the rest of the CIE (to ~30 m; Fig. 2A). Between ~40 m and 90 m, $^{187}Os/^{188}Os_i$ is broadly constant at ~0.34 (Fig. 2A). In detail, the increase in $^{187}Os/^{188}Os_i$ from unradiogenic values close to the CIE onset (–14.5 m) to the highest (more radiogenic) values at 1.45 m closely mirrors changes in $\delta^{13}C_{org}$ (Fig. 2B). Notably, $\delta^{13}C_{org}$ and $^{187}Os/^{188}Os_i$ strongly negatively correlate over this interval (r^2 = 0.93, p-value <0.0001; Fig. 2C). Below and above this interval, there is no correlation between $\delta^{13}C_{org}$ and $^{187}Os/^{188}Os_i$ (Fig. 2C).

The overall decrease in $\delta^{13}C_{org}$ between –14.5 m and 1.45 m comprises two abrupt shifts in $\delta^{13}C_{org}$ of –2.3‰ and –2.9‰ that each occur over a few centimeters of strata (*a* and *b* in Fig. 2B). These two shifts are associated with pronounced increases in $^{187}Os/^{188}Os_i$ of 0.09 (0.31 to 0.40) and 0.15 (0.40 to 0.55), respectively (Fig. 2B). Shift *a* is coincident with a thin (~18 cm) brecciated interval likely associated with a minor fault (strata on either side of the interval belong to the same ammonite zone; Izumi et al., 2018a). Shift *b* spans ~5 cm, and there is no sedimentological evidence for a fault or hiatus. Previous work has demonstrated that both shift *b* and the stratigraphic interval encompassed by shift *a* can be correlated with abrupt shifts through the CIE onset recognized globally (Izumi et al., 2018a).

DISCUSSION AND CONCLUSIONS

The $^{187}Os/^{188}Os_i$ record at Sakuraguchi-dani is similar to the record from the East Tributary of Bighorn Creek, Canada (hereafter 'East Tributary'; Them et al., 2017a; Fig. 3), which was situated on the opposite margin of Panthalassa (Fig. 1). There is no evidence for water-mass restriction in either succession, and the close match in the pattern and magnitude of large-scale $^{187}Os/^{188}Os_i$ changes in both sections strongly

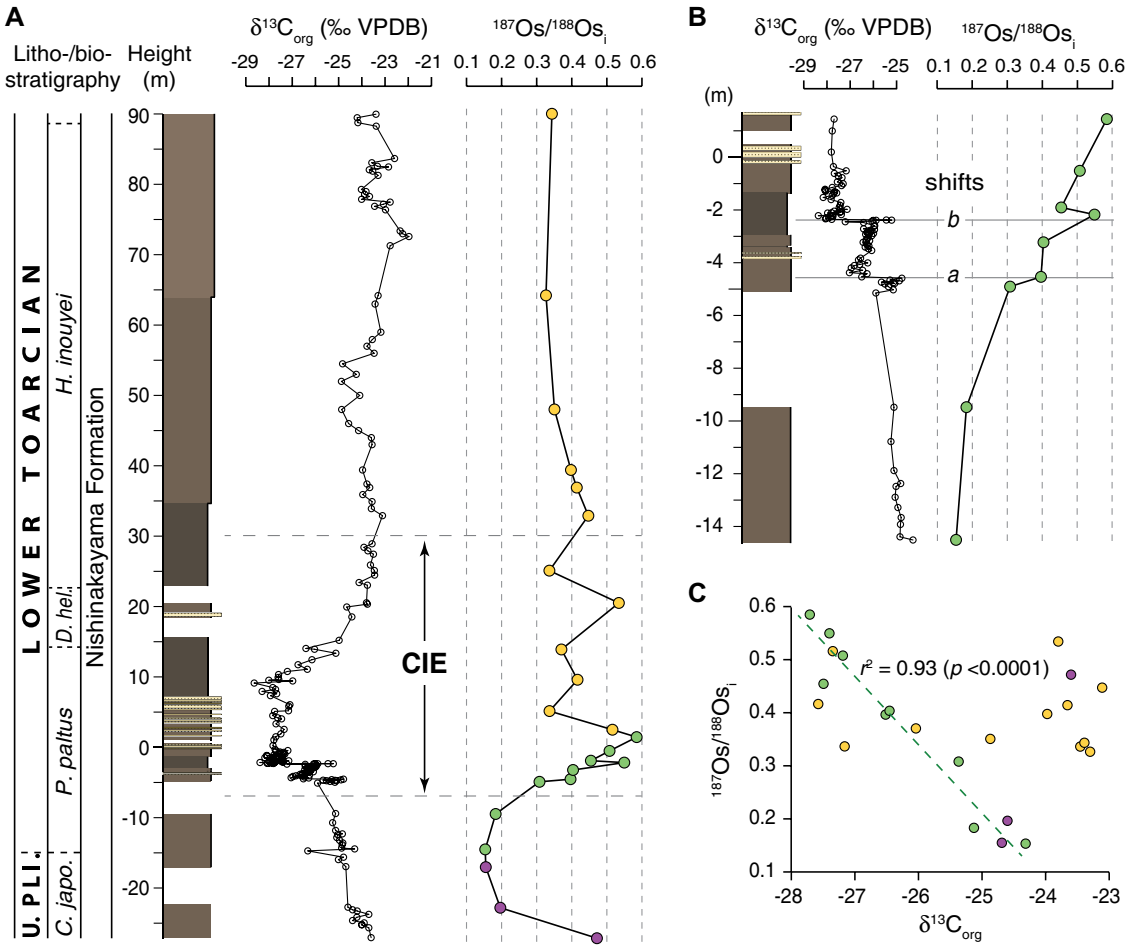

Figure 2. Os-isotope and organic $\delta^{13}C$ ($\delta^{13}C_{org}$) through the Sakuraguchi-dani succession, Japan. (A) Sedimentary log with $^{187}Os/^{188}Os_i$ (i—initial) and $\delta^{13}C_{org}$ variations against lithostratigraphy and ammonite zones (*C. japo.—Canavaria japonica*; *P. paltus—Paltarpites paltus*; *D. hel.—Dactylioceras helianthoides*; *H. inouyei—Harpoceras inouyei*). Color-coding divides $^{187}Os/^{188}Os_i$ data into pre–carbon-isotope excursion (CIE) data (purple), data primarily through onset of the CIE (minimum to maximum $^{187}Os/^{188}Os_i$, green), and data above these (orange). Log is from Izumi et al. (2012, 2018a) and field observations. $\delta^{13}C_{org}$ is from Izumi et al. (2012, 2018a, 2018b), Kemp and Izumi (2014), and this study. PLI.—Pliensbachian; VPDB—Vienna Peedee belemnite. (B) Close-up of the CIE onset, showing abrupt shifts in $^{187}Os/^{188}Os_i$ across $\delta^{13}C_{org}$ shifts *a* and *b*. (C) Cross-plot of $^{187}Os/^{188}Os_i$ and $\delta^{13}C_{org}$ showing the negative correlation between $^{187}Os/^{188}Os_i$ and $\delta^{13}C_{org}$ across the onset of the CIE/$^{187}Os/^{188}Os_i$ excursion, and no correlation below and above this interval.

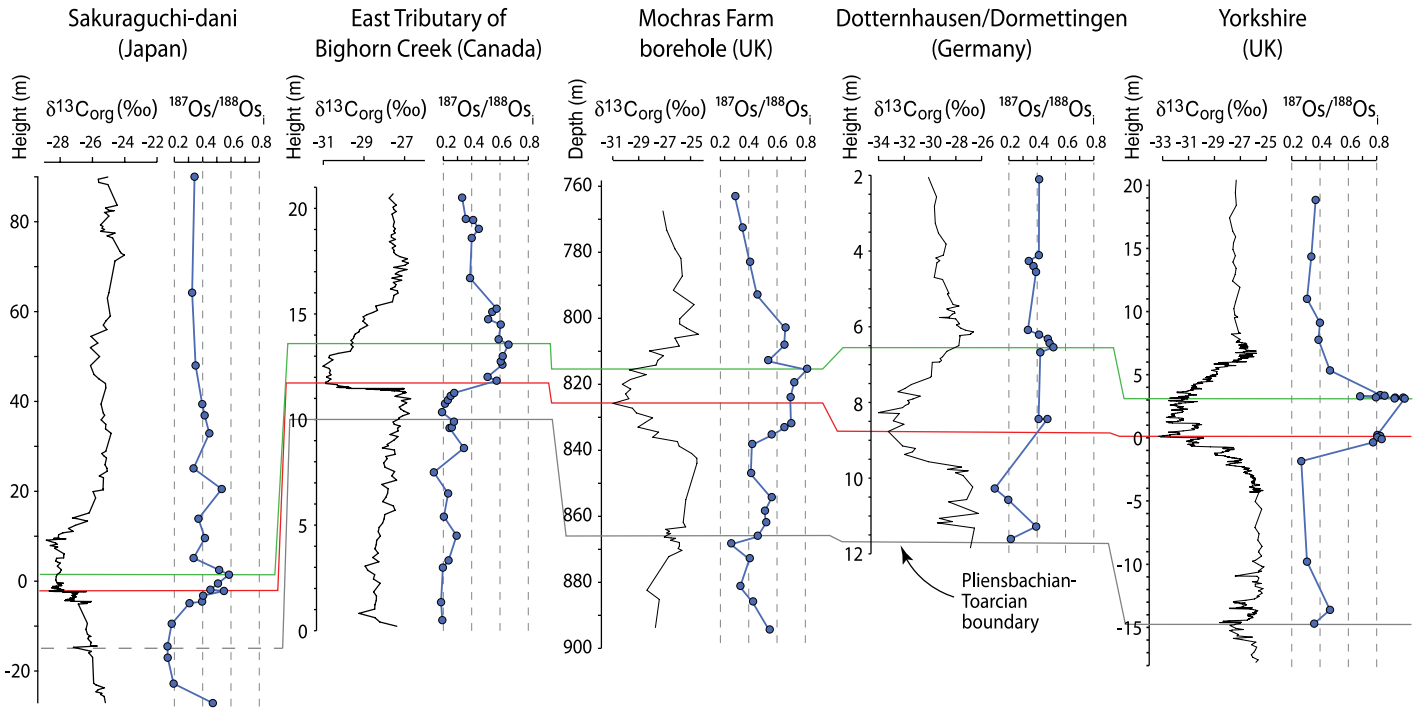

Figure 3. Toarcian organic $\delta^{13}C$ ($\delta^{13}C_{org}$) and $^{187}Os/^{188}Os_i$ (i—initial) records. Tie lines correlate the Pliensbachian-Toarcian boundary (black line), the end of carbon-isotope excursion (CIE) onset (red line), and the $^{187}Os/^{188}Os_i$ maxima (green line) in each section. Heights/depths in each section are taken from the published sources. For Sakuraguchi-dani (Japan), $^{187}Os/^{188}Os_i$ data are from this study, and $\delta^{13}C_{org}$ data are from Izumi et al. (2012, 2018a, 2018b), Kemp and Izumi (2014), and this study (see Table S1 [see footnote 1]). For East Tributary, Canada, $^{187}Os/^{188}Os_i$ data are from Them et al. (2017a) and $\delta^{13}C_{org}$ data are from Them et al. (2017b). For Mochras Farm (UK), $^{187}Os/^{188}Os_i$ and $\delta^{13}C_{org}$ data are from Percival et al. (2016). For Germany, $^{187}Os/^{188}Os_i$ data are from van Acken et al. (2019) (Dormettingen quarry), and $\delta^{13}C_{org}$ data are from Röhl et al. (2001) (Dotternhausen quarry); Dormettingen-Dotternhausen correlation is from van Acken et al. (2019). For Yorkshire (UK), $^{187}Os/^{188}Os_i$ data are from Cohen et al. (2004), and $\delta^{13}C_{org}$ data are from Cohen et al. (2004), Kemp et al. (2005), and Littler et al. (2010). All $\delta^{13}C_{org}$ data are relative to Vienna Peedee belemnite (VPDB).

suggests that these variations reflect changes in the composition of global seawater Os. No correlation exists between detrital proxies (Zr, Al, Ti) and $^{187}Os/^{188}Os_i$ at Sakuraguchi-dani, further emphasizing the predominantly hydrogenous nature of the measured Os (Fig. S1 in the Supplemental Material). Nevertheless, the occurrence of volcanic ashes at Sakuraguchi-dani (Izumi et al., 2012) means that we cannot rule out possible local influence of dissolved unradiogenic Os entering the basin, perhaps accounting for the intermittent low $^{187}Os/^{188}Os_i$ values between 5.15 m and 25.1 m that are not apparent in the East Tributary data (Them et al., 2017a; Fig. 3). This possibility notwithstanding, our data and the data from East Tributary are only weakly similar to $^{187}Os/^{188}Os_i$ data from Europe (Cohen et al., 2004; Percival et al., 2016; van Acken et al., 2019; Fig. 3). Post-CIE $^{187}Os/^{188}Os_i$ values of ~0.3–0.4 occur in all sections, but variable hydrographic restriction in European epicontinental basins may have caused $^{187}Os/^{188}Os$ to evolve to values partly reflective of local Os inputs, particularly during the CIE (McArthur et al., 2008; Them et al., 2017a).

The high resolution of our sampling and the thickness of the Sakuraguchi-dani section allows us to infer a geologically synchronous coupling between carbon release and weathering. Through the onset of the CIE, which may have spanned ~200 k.y. (e.g., Ruebsam et al., 2019), ~93% of the variance in $^{187}Os/^{188}Os_i$ can be explained by changes in $\delta^{13}C_{org}$ driven by carbon release (Fig. 2C). As noted above, abrupt negative shifts in $\delta^{13}C_{org}$ during the CIE onset at Sakuraguchi-dani (shifts *a* and *b* in Fig. 2B) and recognized globally have been interpreted as being due to astronomically controlled hydrate melting or terrestrial carbon-release events that occurred over just a few thousand years each (Kemp et al., 2005; Them et al., 2017b; Izumi et al., 2018a; Ruebsam et al., 2019). The tight correlation and direct correspondence between these carbon-release events and increases in $^{187}Os/^{188}Os_i$ suggest that global weathering responded to carbon inputs on similar time scales. The rapid response of seawater $^{187}Os/^{188}Os$ to flux changes suggests that the seawater residence time of Os was comparable to the time scale of carbon release. Modern Os residence-time estimates are variable (10^3–10^4 yr; e.g., Georg et al., 2013; Rooney et al., 2016); we note that a short Toarcian residence time is consistent with an increase in the burial flux of Os related to expansion of anoxia during the T-OAE (Them et al., 2017a).

Quantifying the magnitude of the weathering increase through the T-OAE, both overall and across abrupt $\delta^{13}C$ shifts *a* and *b*, is complicated because the change in $^{187}Os/^{188}Os_i$ (as controlled by changes in the flux and/or isotopic value of Os delivered to the ocean) has no unique solution. Mass-balance calculations based purely on Os fluxes by Them et al. (2017a) indicated that a 500% increase in continental crust weathering rate would have been required to drive the overall $^{187}Os/^{188}Os_i$ shift at East Tributary (0.25–0.6), assuming modern mantle and continental crust $^{187}Os/^{188}Os$ values of 0.12 and 1.4, respectively. Our pre-CIE $^{187}Os/^{188}Os_i$ value of ~0.2 (Fig. 2), which is also consistent with the lowest pre-CIE values in East Tributary (Fig. 3), adjusts this estimate to ~800% (scenario 1 in Fig. 4A). An increase of this magnitude is unlikely (Percival et al., 2016; Them et al., 2017a) and conflicts with an independent estimate of a ~500% increase in global weathering rate based on Ca isotopes (Brazier et al., 2015).

Smaller weathering-rate increases can be invoked if unradiogenic Os fluxes decreased or if crustal $^{187}Os/^{188}Os$ increased (e.g., Them et al., 2017a). A pre-CIE $^{187}Os/^{188}Os_i$ value of ~0.2 indicates that the flux of mantle-derived unradiogenic Os overwhelmed any radiogenic Os flux. Some of this unradiogenic Os could have derived from basalts erupted as part of the Karoo large igneous province (present-day southern Africa) across the Pliensbachian-Toarcian boundary and leading up to the CIE (Moulin et al., 2017; Ruebsam et al., 2019; Xu

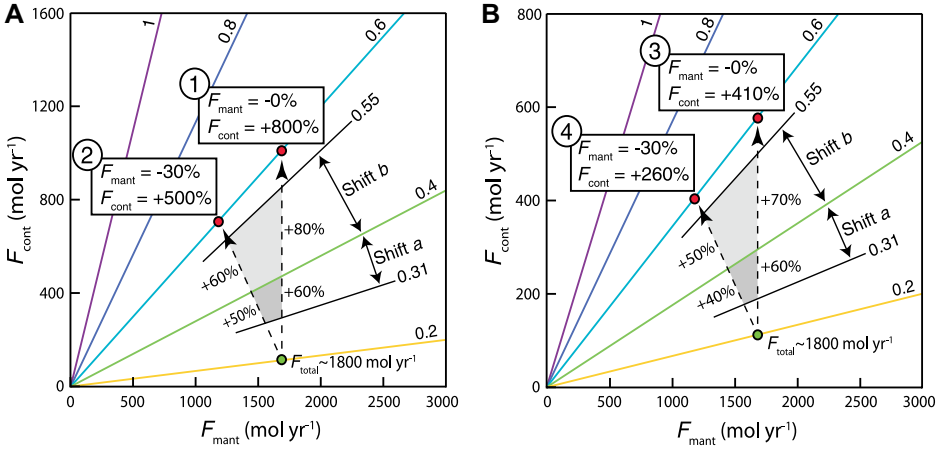

Figure 4. Parameter-space plots illustrating possible changes in radiogenic (F_{cont}, continental crust) and unradiogenic (F_{mant}, mantle) fluxes that could account for the 0.2–0.6 rise in $^{187}Os/^{188}Os_i$ (i—initial) at Sakuraguchi-dani, Japan (Fig. 2). $^{187}Os/^{188}Os_i$ contours (colored lines) are based on the mass balance of seawater $^{187}Os/^{188}Os$; i.e., $^{187}Os/^{188}Os = [(F_{cont} \times N_{cont}) + (F_{mant} \times N_{mant})]/F_{total}$, where N_{cont} and N_{mant} are end-member $^{187}Os/^{188}Os$ compositions of 1.4 (rising to 2 in case of scenarios 3 and 4; scenarios indicated by circled numbers) and 0.12, respectively. The pre–carbon-isotope excursion value (0.2) is, for convenience, based on modern total Os flux (F_{total}) of 1800 mol yr^{-1} (e.g., Georg et al., 2013). (A) Scenario 1 assumes that the overall 0.2–0.6 shift in $^{187}Os/^{188}Os_i$ across the early Toarcian oceanic anoxic event results solely from an increase in F_{cont} (i.e., continental crust weathering) with a modern $^{187}Os/^{188}Os$ value (N_{cont}) of 1.4. Scenario 2 assumes a concomitant ~30% decrease in F_{mant}. (B) Scenarios 3 and 4 assume an instantaneous increase in N_{cont} from 1.4 to 2 at the start of the $^{187}Os/^{188}Os_i$ rise. Gray shaded areas show the changes in F_{mant} and F_{cont} (or just F_{cont}) required to drive abrupt 0.09 and 0.15 changes in $^{187}Os/^{188}Os_i$ across the $\delta^{13}C_{org}$ shifts *a* and *b*, respectively (Fig. 2B). All scenarios require F_{cont} increases of between ~40% and ~80% across these shifts. Calculations assume instantaneous equilibration of Os in seawater, based on the assumed short residence time (see text for details). Mass balance ignores likely minor and invariant Os inputs from other sources, such as cosmic dust.

et al., 2018a; Fig. S2). Karoo volcanism was multi-phased and pulsed (Moulin et al., 2017), and basalts weather rapidly after eruption (e.g., Li et al., 2016). It is thus possible that a decrease in basalt weathering–derived unradiogenic Os flux contributed to the overall $^{187}Os/^{188}Os_i$ rise through the T-OAE. Any decrease was likely only modest given the persistence of Karoo and Ferrar (present-day Antarctica) volcanism through the T-OAE (e.g., Moulin et al., 2017) and the low weatherability of these high-latitude basalts (Them et al., 2017a). Nevertheless, an overall decrease in unradiogenic Os flux across the T-OAE is consistent with data from all sections indicating that $^{187}Os/^{188}Os_i$ remains high after the event, and maxima in $^{187}Os/^{188}Os_i$ occur after the end of the CIE onset, and thus perhaps after cessation of carbon release (Fig. 3). A ~30% decrease in unradiogenic Os flux would be needed to reconcile the Sakuraguchi-dani $^{187}Os/^{188}Os_i$ record with the ~500% weathering-increase estimate of Brazier et al. (2015) (scenario 2 in Fig. 4A). A smaller or negligible decrease in unradiogenic flux, and smaller weathering increases, can be invoked if the onset of the T-OAE was accompanied by weathering of ^{187}Os-enriched organic-rich rocks and/or sulfides (e.g., Them et al., 2017a). A rise in crustal $^{187}Os/^{188}Os$ from 1.4 to 2 at the start of the CIE would necessitate an ~410% increase in continental weathering to explain the Sakuraguchi-dani data, or ~260% if a coeval decrease in unradiogenic Os flux occurred (scenarios 3 and 4, respectively, in Fig. 4B). A value of ~2 is a probable upper limit on global continental crust $^{187}Os/^{188}Os$ (Cohen et al., 2004; Them et al., 2017a).

Regardless of the overall magnitude of the weathering increase across the T-OAE, the marked increases in $^{187}Os/^{188}Os_i$ across the inferred rapid carbon-release events at $\delta^{13}C_{org}$ shifts *a* and *b* imply abrupt increases in weathering. The broad mass-balance constraints explored above suggest that these carbon-release events were associated with increases in radiogenic Os inputs of between ~40% (shift *a*, scenario 4) and ~80% (shift *b*, scenario 1), assuming instantaneous equilibration of seawater $^{187}Os/^{188}Os$ and no change in mantle or crust $^{187}Os/^{188}Os$ across the shifts themselves (Fig. 4). The larger of the two $\delta^{13}C_{org}$ shifts (shift *b*) spans 5 cm of strata and has been attributed to a carbon-release event with an estimated time scale of <2 k.y. (Izumi et al., 2018a). The maximum of the coeval $^{187}Os/^{188}Os_i$ increase (0.55) occurs 16 cm above the end of this $\delta^{13}C_{org}$ shift. This suggests that the weathering increase associated with this carbon-release event (~50% to ~80%; Fig. 4) occurred over a comparable time scale (an inference also supported by the short residence time of seawater Os relative to carbon). On such short time scales, runoff may be a key limiting factor controlling rapid and large-scale Os flux to the ocean (Dosseto et al., 2015; Eiriksdottir et al., 2011; Bastian et al., 2017), and there is widespread evidence that tropical precipitation, runoff, and fluvial power all increased contemporaneously with carbon release and/or warming during the T-OAE (Izumi et al., 2018a; Xu et al., 2018b; Kemp et al., 2019).

ACKNOWLEDGMENTS

Kemp was supported by the National Natural Science Foundation of China (grant 41888101), the National Recruitment Program for Young Professionals (P.R. China), the UK Natural Environment Research Council (NERC) (grant NE/I02089X/1), and the Great Britain Sasakawa and Daiwa Anglo-Japanese Foundations. Selby acknowledges A. Hofmann, G. Nowell, and C. Ottley, a TOTAL Endowment Fund, and a China University of Geosciences (Wuhan) Dida Scholarship. Izumi acknowledges the Japan Society for the Promotion of Science (JSPS) (grants KAKENHI 12J08818 and 15J08821). This study contributes to International Geoscience Programme (IGCP) Project 655 (IUGS-UNESCO). We thank three reviewers for their careful assessment of our work.

REFERENCES CITED

Bastian, L., Revel, M., Bayon, G., Dufour, A., and Vigier, N., 2017, Abrupt response of chemical weathering to Late Quaternary hydroclimate changes in northeast Africa: Scientific Reports, v. 7, 44231, https://doi.org/10.1038/srep44231.

Brazier, J.-M., Suan, G., Tacail, T., Simon, L., Martin, J.E., Mattioli, E., and Balter, V., 2015, Calcium isotope evidence for dramatic increase of continental weathering during the Toarcian oceanic anoxic event (Early Jurassic): Earth and Planetary Science Letters, v. 411, p. 164–176, https://doi.org/10.1016/j.epsl.2014.11.028.

Cohen, A.S., Coe, A.L., Harding, S.M., and Schwark, L., 2004, Osmium isotope evidence for the regulation of atmospheric CO_2 by continental weathering: Geology, v. 32, p. 157–160, https://doi.org/10.1130/G20158.1.

Dosseto, A., Vigier, N., Joannes-Boyau, R., Moffat, I., Singh, T., and Srivastava, P., 2015, Rapid response of silicate weathering rates to climate change in the Himalaya: Geochemical Perspectives Letters, v. 1, p. 10–19, https://doi.org/10.7185/geochemlet.1502.

Eiriksdottir, E.S., Gislason, S.R., and Oelkers, E.H., 2011, Does runoff or temperature control chemical weathering rates?: Applied Geochemistry, v. 26, p. S346–S349, https://doi.org/10.1016/j.apgeochem.2011.03.056.

Georg, R.B., West, A.J., Vance, D., Newman, K., and Halliday, A.N., 2013, Is the marine isotope record a probe for CO_2 release from sedimentary rocks?: Earth and Planetary Science Letters, v. 367, p. 28–38, https://doi.org/10.1016/j.epsl.2013.02.018.

Hesselbo, S.P., and Pieńkowski, G., 2011, Stepwise atmospheric carbon-isotope excursion during the Toarcian Oceanic Anoxic Event (Early Jurassic, Polish Basin): Earth and Planetary Science Letters, v. 301, p. 365–372, https://doi.org/10.1016/j.epsl.2010.11.021.

Hesselbo, S.P., Gröcke, D.R., Jenkyns, H.C., Bjerrum, C.J., Farrimond, P., Morgans Bell, H.S., and Green, O.R., 2000, Massive dissociation of gas hydrate during a Jurassic oceanic event: Nature, v. 406, p. 392–395, https://doi.org/10.1038/35019044.

Izumi, K., Miyaji, T., and Tanabe, K., 2012, Early Toarcian (Early Jurassic) oceanic anoxic event

recorded in the shelf deposits in the northwestern Panthalassa: Evidence from the Nishinakayama Formation in the Toyora area, west Japan: Palaeogeography, Palaeoclimatology, Palaeoecology, v. 315–316, p. 100–108, https://doi.org/10.1016/j.palaeo.2011.11.016.

Izumi, K., Kemp, D.B., Itamiya, S., and Inui, M., 2018a, Sedimentary evidence for enhanced hydrological cycling in response to rapid carbon release during the early Toarcian oceanic anoxic event: Earth and Planetary Science Letters, v. 481, p. 162–170, https://doi.org/10.1016/j.epsl.2017.10.030.

Izumi, K., Endo, K., Kemp, D.B., and Inui, M., 2018b, Oceanic redox conditions through the late Pliensbachian to early Toarcian on the northwestern Panthalassa margin: Insights from pyrite and geochemical data: Palaeogeography, Palaeoclimatology, Palaeoecology, v. 493, p. 1–10, https://doi.org/10.1016/j.palaeo.2017.12.024.

Kemp, D.B., and Izumi, K., 2014, Multiproxy geochemical analysis of a Panthalassic margin record of the early Toarcian oceanic anoxic event (Toyora area, Japan): Palaeogeography, Palaeoclimatology, Palaeoecology, v. 414, p. 332–341, https://doi.org/10.1016/j.palaeo.2014.09.019.

Kemp, D.B., Coe, A.L., Cohen, A.S., and Schwark, L., 2005, Astronomical pacing of methane release in the Early Jurassic period: Nature, v. 437, p. 396–399, https://doi.org/10.1038/nature04037.

Kemp, D.B., Baranyi, V., Izumi, K., and Burgess, R.D., 2019, Organic matter variations and links to climate change across the early Toarcian oceanic anoxic event (T-OAE) in Toyora area, southwest Japan: Palaeogeography, Palaeoclimatology, Palaeoecology, v. 530, p. 90–102, https://doi.org/10.1016/j.palaeo.2019.05.040.

Li, G., et al., 2016, Temperature dependence of basalt weathering: Earth and Planetary Science Letters, v. 443, p. 59–69, https://doi.org/10.1016/j.epsl.2016.03.015.

Littler, K., Hesselbo, S.P., and Jenkyns, H.C., 2010, A carbon-isotope perturbation at the Pliensbachian-Toarcian boundary: Evidence from the Lias Group, NE England: Geological Magazine, v. 147, p. 181–192, https://doi.org/10.1017/S0016756809990458.

McArthur, J.M., Algeo, T.J., van de Schootbrugge, B., Li, Q., and Howarth, R.J., 2008, Basinal restriction, black shales, Re-Os dating, and the early Toarcian (Jurassic) oceanic anoxic event: Paleoceanography, v. 23, PA4217, https://doi.org/10.1029/2008PA001607.

McElwain, J.C., Wade-Murphy, J., and Hesselbo, S.P., 2005, Changes in carbon dioxide during an oceanic anoxic event linked to intrusion into Gondwana coals: Nature, v. 435, p. 479–482, https://doi.org/10.1038/nature03618.

Moulin, M., Fluteau, F., Courtillot, V., Marsh, J., Delpech, G., Quidelleur, X., and Gérard, M., 2017, Eruptive history of the Karoo lava flows and their impact on early Jurassic environmental change: Journal of Geophysical Research: Solid Earth, v. 122, p. 738–772, https://doi.org/10.1002/2016JB013354.

Percival, L.M.E., Cohen, A.S., Davies, M.K., Dickson, A.J., Hesselbo, S.P., Jenkyns, H.C., Leng, M.J., Mather, T.A., Storm, M.S., and Xu, W., 2016, Osmium isotope evidence for two pulses of increased continental weathering linked to Early Jurassic volcanism and climate change: Geology, v. 44, p. 759–762, https://doi.org/10.1130/G37997.1.

Röhl, H.-J., Schmid-Röhl, A., Oschmann, W., Frimmel, A., and Schwark, L., 2001, Erratum to "The Posidonia Shale (Lower Toarcian) of SW-Germany: An oxygen-depleted ecosystem controlled by sea level and palaeoclimate": Palaeogeography, Palaeoclimatology, Palaeoecology, v. 169, p. 273–299, https://doi.org/10.1016/S0031-0182(01)00201-2.

Rooney, A.D., Selby, D., Lloyd, J.M., Roberts, D.H., Lückge, A., Sageman, B.B., and Prouty, N.G., 2016, Tracking millennial-scale Holocene glacial advance and retreat using osmium isotopes: Insights from the Greenland ice sheet: Quaternary Science Reviews, v. 138, p. 49–61, https://doi.org/10.1016/j.quascirev.2016.02.021.

Ruebsam, W., Mayer, B., and Schwark, L., 2019, Cryosphere carbon dynamics control early Toarcian global warming and sea level evolution: Global and Planetary Change, v. 172, p. 440–453, https://doi.org/10.1016/j.gloplacha.2018.11.003.

Them, T.R., Gill, B.C., Selby, D., Gröcke, D.R., Friedman, R.M., and Owens, J.D., 2017a, Evidence for rapid weathering response to climatic warming during the Toarcian Oceanic Anoxic Event: Scientific Reports, v. 7, 5003, https://doi.org/10.1038/s41598-017-05307-y.

Them, T.R., Gill, B.C., Caruthers, A.H., Gröcke, D.R., Tulsky, E.T., Martindale, R.C., Poulton, T.P., and Smith, P.L., 2017b, High-resolution carbon isotope records of the Toarcian Oceanic Anoxic Event (Early Jurassic) from North America and implications for the global drivers of the Toarcian carbon cycle: Earth and Planetary Science Letters, v. 459, p. 118–126, https://doi.org/10.1016/j.epsl.2016.11.021.

van Acken, D., Tütken, T., Daly, J.S., Schmid-Röhl, A., and Orr, P.J., 2019, Rhenium-osmium geochronology of the Toarcian Posidonia Shale, SW Germany, Palaeogeography, Palaeoclimatology: Palaeoecology, v. 534, https://doi.org/10.1016/j.palaeo.2019.109294.

Xu, W., Mac Niocaill, C., Ruhl, Jenkyns, H.C., Riding, J.B., and Hesselbo, S.P., 2018a, Magnetostratigraphy of the Toarcian Stage (Lower Jurassic) of the Llanbedr (Mochras Farm) Borehole, Wales: Basis for a global standard and implications for volcanic forcing of palaeoenvironmental change: Journal of the Geological Society, v. 175, p. 594–604, https://doi.org/10.1144/jgs2017-120.

Xu, W., et al., 2018b, Evolution of the Toarcian (Early Jurassic) carbon-cycle and global climatic controls on local sedimentary processes (Cardigan Bay Basin, UK): Earth and Planetary Science Letters, v. 484, p. 396–411, https://doi.org/10.1016/j.epsl.2017.12.037.

Printed in USA